INTERNATIONAL JOURNAL OF FLUID POWER, 2016
VOL. 17, NO. 3, 163–172
http://dx.doi.org/10.1080/14399776.2016.1185876

Taylor & Francis
Taylor & Francis Group

Model-based force and position tracking control of an asymmetric cylinder with a digital hydraulic valve

Matti Linjama, Mikko Huova and Kalevi Huhtala

Department of Intelligent Hydraulics and Automation, Tampere University of Technology, Tampere, Finland

ABSTRACT

This paper presents a model-based control solution for large inertia systems controlled by a fast digital hydraulic valve. The solution is based on model-based force control and it is shown that the cylinder chamber pressures have first order dynamics with the proper parameter selection. The robust stability is analyzed under unknown load mass, bulk modulus, and delay, and it is shown that a simple cascaded P + PID controller results in good control performance and robustness. The simulated results show smooth and stable response with good tracking performance despite large variations in the load mass and bulk modulus.

ARTICLE HISTORY
Received 22 June 2015
Accepted 25 April 2016

KEYWORDS
Digital hydraulics; tracking control; force control; position control

1. Introduction

Electrohydraulic servo systems are used in many applications, such as aircraft actuators and paper mills, because of their high power-to-weight ratio. Position, velocity and force control are the basic functions of modern hydraulic actuators (Jelali and Kroll 2004). The compressibility of the fluid and the non-linear flow characteristics of the control valves make these systems difficult to control, and several different approaches have been suggested for controlling force, velocity, and position tracking. Kim *et al.* (2015) studied flatness based non-linear control and demonstrated an approximate 0.3 mm position tracking error with a peak velocity of 63 mm/s. Thus, the commonly used performance index – the maximum error divided by the peak velocity (Zhu and Vukovich 2011) – was about 0.005 s. Koivumäki and Mattila (2015) used virtual decomposition control in a construction crane and achieved a performance index of 0.0030 s. Won *et al.* (2015) used the high-gain disturbance observer in the control of 1-DOF hydraulic arm and experimental results demonstrated performance index of about 0.005 s. Eryilmaz and Wilson (2001) designed a controller using the singular perturbation theory and Lyapunov-type nonlinear feedback. The most interesting benefits of their solution are its robustness against variations in the bulk modulus and the absence of the need to differentiate velocity or pressures. The simulated results showed a performance index of 0.0008 s, but the load mass was only 12 kg.

Digital hydraulic valve control is a potential alternative for traditional hydraulic servo systems (Linjama and Vilenius 2005, Linjama *et al.* 2008). The basic layout of a digital hydraulic four-way valve is shown in Figure 1. It consists of four valve series, which are also known as a digital flow control unit (DFCU), to control each flow path independently. Each DFCU has 2^N opening combinations where N is the number of parallel connected valves; thus, the four-way valve has 2^{4N} opening combinations. The typical value for N is five, so the number of opening combinations is over one million. Another approach is to use mutually similar valves, which results in $N + 1$ opening combinations with N parallel connected valves (Linjama and Vilenius 2008). Model-based control has been used to determine the optimal opening combination (Linjama and Vilenius 2005). The steady state model has been used and the intrinsic assumption is that the system dynamics is fast in comparison to the sampling period of the controller. However, that assumption is not valid in systems with large inertia.

This paper presents a model-based control solution for large inertia systems controlled by a fast digital hydraulic valve. The solution is based on a model-based force control and the outcome shows that the cylinder chamber pressures have first order dynamics with the proper parameter selection. The robust stability was analyzed under unknown load mass, bulk modulus, and delay, and it was shown that a simple cascaded P + PID controller results in good control performance

CONTACT Matti Linjama matti.linjama@tut.fi

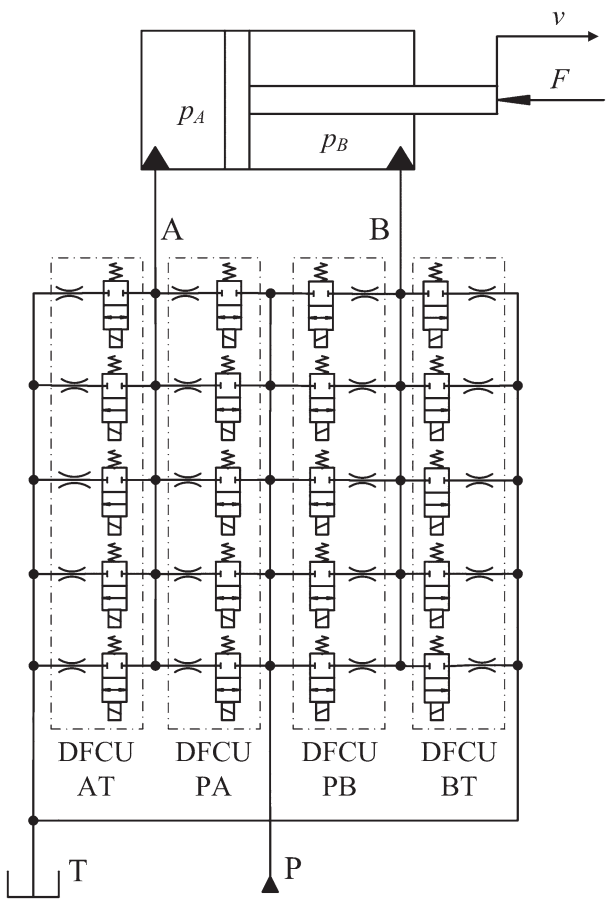

Figure 1. Digital valve system with five parallel connected valves. Orifices are used to adjust the flow capacity of the valves according to binary series.

and robustness. The simulated results show smooth and stable response with good tracking performance despite large variations in the load mass. A performance index of 0.0032 s was achieved, which is the same level that was obtained using more complicated controllers as shown in the work of Kim *et al.* (2015), Koivumäki and Mattila (2015) and Won *et al.* (2015).

2. Model-based control of an asymmetric cylinder

2.1. System model

The dynamics of a hydraulic cylinder with inertia m and external force F_{load} can be expressed as:

$$\begin{aligned}\dot{p}_A &= \frac{B_A}{A_A x + V_{0A}}\left(Q_{PA} - Q_{AT} - A_A\dot{x}\right)\\ \dot{p}_B &= \frac{B_B}{A_B\left(x_{\max} - x\right) + V_{0B}}\left(Q_{PB} - Q_{BT} + A_B\dot{x}\right)\\ m\ddot{x} &= p_A A_A - p_B A_B - F_\mu(\dot{x}) - F_{\text{load}}\end{aligned} \tag{1}$$

The flow rates of DFCUs are modelled using the generalised turbulent flow model with cavitation choking (Linjama *et al.* 2012):

$$Q_{XY,i} = \begin{cases} \mathbf{K_{v,XY}}(i)\left(p_X - p_Y\right)^{\mathbf{x_{XY}}(i)}, & \mathbf{b_{XY}}(i)p_X < p_Y \le p_X \\ \mathbf{K_{v,XY}}(i)\left[\left(1-\mathbf{b_{XY}}(i)\right)p_X\right]^{\mathbf{x_{XY}}(i)}, & p_Y \le \mathbf{b_{XY}}(i)p_X \\ -\mathbf{K_{v,XY}}(i)\left(p_Y - p_X\right)^{\mathbf{x_{XY}}(i)}, & \mathbf{b_{XY}}(i)p_Y < p_X < p_Y \\ -\mathbf{K_{v,XY}}(i)\left[\left(1-\mathbf{b_{XY}}(i)\right)p_Y\right]^{\mathbf{x_{XY}}(i)}, & p_X \le \mathbf{b_{XY}}(i)p_Y \end{cases} \tag{2}$$

$$Q_{XY} = \sum_{i=1}^{N} \mathbf{u_{XY}}(i)Q_{XY,i}$$

where XY is either PA, AT, PB, or BT and $\bullet(i)$ refers to the i:th element of the vector. Combining Equations 1 and 2 gives three non-linear differential equations:

$$\begin{aligned}\dot{p}_A &= f_A\left(p_A, x, \dot{x}, \mathbf{u_{PA}}, \mathbf{u_{AT}}, p_P, p_T\right)\\ \dot{p}_B &= f_B\left(p_B, x, \dot{x}, \mathbf{u_{PB}}, \mathbf{u_{BT}}, p_P, p_T\right)\\ \ddot{x} &= f_x\left(p_A, p_B, \dot{x}, F_{\text{load}}\right)\end{aligned} \tag{3}$$

The control inputs of the system are the control vectors of the DFCUs ($\mathbf{u_{PA}}$, $\mathbf{u_{AT}}$, $\mathbf{u_{PB}}$, $\mathbf{u_{BT}}$) and the disturbances are supply pressure p_P, tank pressure p_T, and load force F_{load}. The state variables are chamber pressures p_A and p_B as well as piston position x and velocity $\dot{x}$.

2.2. One-step ahead estimator

The assumption made in this paper is that the inertia m is so large that the velocity does not change significantly during one controller sampling period. This decouples the differential equations and makes it possible to estimate pressures using scalar integration methods without knowledge of the inertia. Heun's method is used for estimating the pressure changes (Goode 2000, p. 86):

$$\begin{aligned}\tilde{p}_A(k+1) = {} & p_A(k) + T_S f_A(p_A(k), x(k), \dot{x}(k), \mathbf{u_{PA}}(k), \mathbf{u_{AT}}(k), p_P(k), p_T(k))\\ \hat{p}_A(k+1) = {} & p_A(k) + \tfrac{T_S}{2}\big(f_A(p_A(k), x(k), \dot{x}(k), \mathbf{u_{PA}}(k), \mathbf{u_{AT}}(k), p_P(k), p_T(k))\\ & + f_A(\tilde{p}_A(k+1), x(k) + T_S\dot{x}(k), \dot{x}(k), \mathbf{u_{PA}}(k), \mathbf{u_{AT}}(k), p_P(k), p_T(k))\big)\end{aligned} \tag{4}$$

The equations for the B-side pressure are similar.

2.3. Inner-loop force controller

The chamber pressures can be controlled by selecting the control signals so that the differences between the target pressures and the estimated pressures are minimised. The output of the hydraulic cylinder is piston force, which is given by:

$$F = p_A A_A - p_B A_B - F_\mu \tag{5}$$

Thus, there are two control variables and one output. One possible option is that the pressure differentials over the DFCUs are the same:

$$
\begin{aligned}
&p_P - p_{A,\mathrm{ref}} = p_{B,\mathrm{ref}} - p_T \\
&F_{\mathrm{ref}} = p_{A,\mathrm{ref}}A_A - p_{B,\mathrm{ref}}A_B = p_{A,\mathrm{ref}}A_A - \left(p_P + p_T - p_{A,\mathrm{ref}}\right)A_B \\
\Rightarrow\ & p_{A,\mathrm{ref}} = \frac{F_{\mathrm{ref}}}{A_A+A_B} + \frac{A_B}{A_A+A_B}\left(p_P + p_T\right) \\
& p_{B,\mathrm{ref}} = \frac{-F_{\mathrm{ref}}}{A_A+A_B} + \frac{A_A}{A_A+A_B}\left(p_P + p_T\right)
\end{aligned} \tag{6}
$$

Equation 6 does not include friction force. If friction compensation is used, it can be added to F_{ref}. The primary objective of the force controller is to minimise the force error while the secondary objective is to keep the pressures near the target values. This is solved by first selecting the N_{cand} control candidates for the A-side and the B-side, so that the estimated error in the chamber pressures is small, and then calculating the force error for each combination of the control candidates. The control candidates are selected according to the weighted sum of the estimated pressure error and the magnitude of the openings of the DFCUs:

$$
\begin{aligned}
J_A &= \left|p_{A,\mathrm{ref}} - \hat{p}_A(k+1)\right| + W_{u,p}\mathbf{b}^{\mathrm{T}}\left(\mathbf{u_{PA}} + \mathbf{u_{AT}}\right) \\
J_B &= \left|p_{B,\mathrm{ref}} - \hat{p}_B(k+1)\right| + W_{u,p}\mathbf{b}^{\mathrm{T}}\left(\mathbf{u_{PB}} + \mathbf{u_{BT}}\right)
\end{aligned} \tag{7}
$$

where $W_{u,p}$ is the weight for the openings of the DFCUs and the vector $\mathbf{b}$ determines the relative sizes of the valves; for example, $\mathbf{b} = [1, 2, 4, 8]^{\mathrm{T}}$ for the binary coded DFCU with four valves. The values of J_A and J_B are calculated for all possible control combinations and the N_{cand} candidates that give the smallest value for J_A and J_B are selected for further analysis. Thus, the total number of candidates is $N_{\mathrm{cand}}{}^2$. The final selection is made by minimising the following penalty function:

$$
\begin{aligned}
J &= \left|F_{\mathrm{ref}} - \hat{F}(k+1)\right| + W_{u,F}\mathbf{b}^{\mathrm{T}}\left(\mathbf{u_{PA}} + \mathbf{u_{AT}} + \mathbf{u_{PB}} + \mathbf{u_{BT}}\right) \\
\hat{F}(k+1) &= \hat{p}_A(k+1)A_A - \hat{p}_B(k+1)A_B
\end{aligned} \tag{8}
$$

2.4. Pressure and force dynamics under an unknown bulk modulus

The inner-loop controller is a non-linear selection scheme that tries to minimise the error between the target pressure and the estimated pressure. In the ideal case, the controller finds the valve openings where the pressure error is small after one sampling period. In practice, error occurs due to the parameter uncertainty of the model and the finite resolution of the DFCUs. The flow rate of the on/off valve (Equation 2) can be calculated reliably for the given pressures (Linjama *et al.* 2012). Much larger uncertainty comes from the uncertainty of the bulk modulus, because it depends on the pressure and the amount of entrapped air. Additional error for the pressure estimate comes from the inaccuracy of the estimator (Equation 4) because simple fixed step integration is used. This error can be reduced by decreasing the sampling period of the controller or by using a multi-step approach. For simplicity, it is assumed that all uncertainty can be lumped into the bulk modulus. It is assumed that the controller works perfectly but the bulk modulus estimate is incorrect. Thus, the estimated pressure equals the target value after one sampling period:

$$
\begin{aligned}
\hat{p}_A(k+1) &= p_A(k) + \int_0^{T_S} \frac{\hat{B}_A}{A_A x + V_{0A}}\left(Q_{PA} - Q_{AT} - A_A\dot{x}\right)dt \\
&= p_{A,\mathrm{ref}}
\end{aligned} \tag{9}
$$

Now, the real pressure dynamics can be expressed as:

$$
\begin{aligned}
p_A(k+1) &= p_A(k) + \int_0^{T_S} \frac{B_A}{A_A x + V_{0A}}\left(Q_{PA} - Q_{AT} - A_A\dot{x}\right)dt \\
&= p_A(k) + \frac{B_A}{\hat{B}_A}\int_0^{T_S} \frac{\hat{B}_A}{A_A x + V_{0A}}\left(Q_{PA} - Q_{AT} - A_A\dot{x}\right)dt
\end{aligned} \tag{10}
$$

Combining Equations 9 and 10 gives the following difference equation for the pressure dynamics:

$$
p_A(k+1) = \left(1 - \frac{B_A}{\hat{B}_A}\right)p_A(k) + \frac{B_A}{\hat{B}_A}p_{A,\mathrm{ref}} \tag{11}
$$

which is stable for $\hat{B}_A > B_A/2$. The optimal response is achieved with $\hat{B}_A = B_A$, and for $\hat{B}_A > B_A$ the response has the first order dynamics with the time constant:

$$
\tau_A = -\frac{T_S}{\ln\left(1 - B_A/\hat{B}_A\right)} \tag{12}
$$

The analysis shows it is safer to use too big value for the estimate of the bulk modulus. Too big value makes the pressure estimation only slower while too small value may yield instability. The tuning is made in such a way that the estimate of the bulk modulus is selected to be the highest possible value, i.e. the bulk modulus of the fluid at the maximum system pressure without any entrapped air. This guarantees that the pressure has the first order dynamics.

The B-side pressure dynamics can be derived in a similar way. The A-side and B-side pressure dynamics can have different time constants because the real bulk moduli can be different. The force dynamics in s-domain is:

$$
\begin{aligned}
F(s) &= A_A p_A(s) - A_B p_B(s) \\
&= \frac{A_A}{\tau_A s + 1}p_{A,\mathrm{ref}} - \frac{A_B}{\tau_B s + 1}p_{B,\mathrm{ref}} \\
&= \frac{\frac{\tau_B A_A + \tau_A A_B}{A_A + A_B}s + 1}{\left(\tau_A s + 1\right)\left(\tau_B s + 1\right)}F_{\mathrm{ref}} \\
&\quad + \frac{A_A A_B}{A_A + A_B}\left(\frac{\left(\tau_B - \tau_A\right)s}{\left(\tau_A s + 1\right)\left(\tau_B s + 1\right)}\right) \\
&\quad \left(p_P(s) + p_T(s)\right) \hat{=} G_F(s)F_{\mathrm{ref}} + G_p(s)\left(p_P(s) + p_T(s)\right)
\end{aligned} \tag{13}
$$

The second term vanishes if the supply and tank pressures are constant.

2.5. The outer-loop velocity controller

The analysis presented in Section 2.4 shows that, with proper selection of the estimate of the bulk modulus, the inner-loop controller has the dynamics $G_F(s)$ with unknown time constants τ_A and τ_B. The upper limit of the time constants can be determined by estimating the lowest possible bulk modulus. For example, if it is assumed that the real bulk modulus is at least half of the estimated value and the sampling period is 10 ms, the time constant is 14.4 ms. The lower limit for the time constants is zero. In addition to the time constants, the system also has delay d caused by the valves, the sampling, the computation, and the pipeline dynamics. The resonances caused by the pipeline dynamics are assumed to be in high frequency range and the controller is tuned to be robust against high frequency modelling errors. This assumption is valid if pipeline lengths are 2 m at maximum. The lowest natural frequency of a 2 m pipeline is about 1800 rad/s, and it will be shown later that the system is robust against such modelling error. The block diagram of the system is shown in Figure 2 in which $G_V(s)$ is the transfer function of the velocity controller. The transfer function of the nominal model is selected to be:

$$G_N(s) = \frac{1}{m_{\min} s} e^{-d_{\min} s} \tag{14}$$

where $m_{\min}$ is the smallest possible load mass of the system and $d_{\min}$ is the minimum delay of the valves. The true transfer function is:

$$G_T(s) = \frac{1}{m\,s} G_F(s) e^{-ds} \tag{15}$$

where m is the actual mass, $G_F(s)$, as given by Equation 13, and d is the actual system delay caused by the sampling, the computation, the valve dynamics, and the pipeline dynamics. The multiplicative error caused by the parameter variations is:

$$\Delta(s) = \frac{G_T(s) - G_N(s)}{G_N(s)} \tag{16}$$

Now, the system remains stable if $G_T(s)$ and $G_N(s)$ have the same number of unstable poles and the following holds (Green and Limebeer 1995):

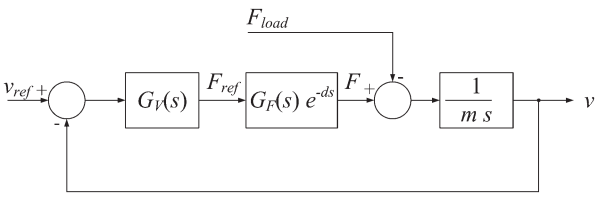

Figure 2. Block diagram of the velocity control system.

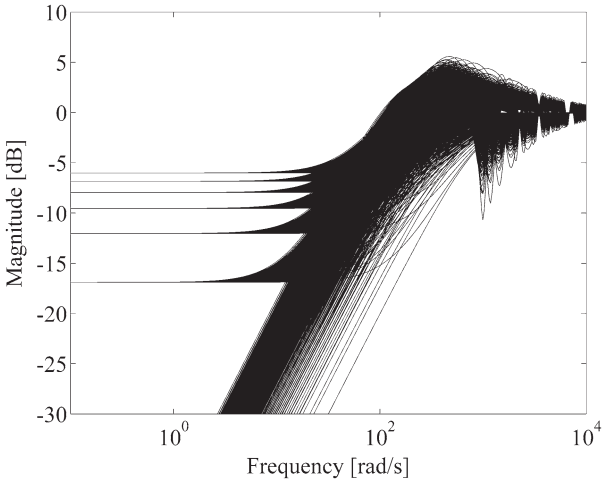

Figure 3. Multiplicative modelling error of the velocity controlled system with m = 250–500 kg, τ_A = 1–6.4 ms, τ_B = 1–6.4 ms, and delay d = 1.5–7 ms.

$$\left|\Delta(j\omega)\right| < \left|\frac{1 + G_N(j\omega)G_V(j\omega)}{G_N(j\omega)G_V(j\omega)}\right| \quad \forall\omega > 0 \tag{17}$$

Both $G_T(s)$ and $G_N(s)$ have one pole at the origin and the other poles are stable. Therefore, the stability criterion of Equation 17 can be used.

Example 1. Figure 3 shows the multiplicative modelling error when $m_{\min}$ is 250 kg, m is 250–500 kg, time constants τ_A and τ_B are 1–6.4 ms, and delay d is 1.5–7 ms. The piston diameter is 40 mm and the piston rod diameter is 20 mm.

Based on Example 1, it can be stated that the multiplicative modelling error is below curve:

$$\Delta_M = K\left|\tau j\omega + 1\right| \tag{18}$$

where the time constant τ is larger than the largest possible value of time constants τ_A and τ_B, and K is a constant smaller than 1. A good property of Δ_M is that it increases with frequency; thus, it takes into account unknown high frequency modelling errors such as pipeline dynamics. The robust controller tuning is such that:

$$\left|\frac{1 + G_N(j\omega)G_V(j\omega)}{G_N(j\omega)G_V(j\omega)}\right| > \Delta_M \quad \forall\omega > 0 \tag{19}$$

One possible controller is the P-controller:

$$G_V(s) = K_{P,\text{vel}} \tag{20}$$

Example 2. Figure 4 shows both sides of Equation 19 for the system presented in Example 1 when $K_{P,\text{vel}}$ is 19000 Ns/m. The parameters of Δ_M are selected to be K = 0.9 and τ = 13 ms. It is seen that the P-controller yields almost an exact fit on Δ_M. Figure 5 shows the velocity step responses of the system with the parameter variations of Example 1. The maximum overshoot is 35% and the worst case settling time is about 0.13 s.

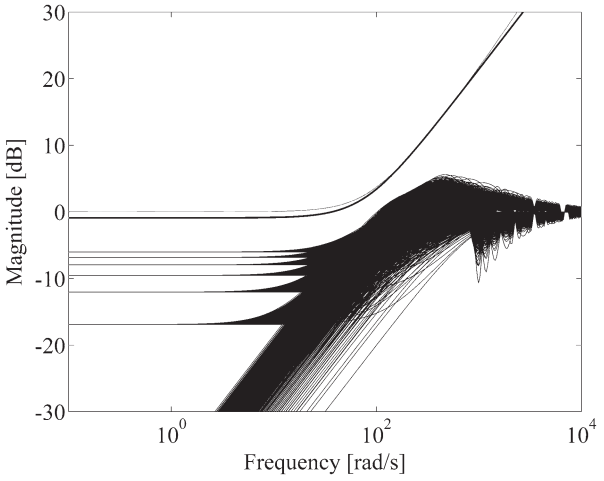

Figure 4. Both sides of Equation (19) with the multiplicative modelling error of Example 1.

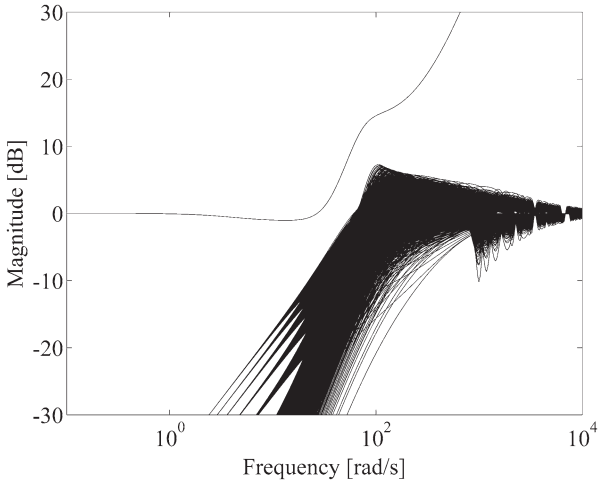

Figure 7. Multiplicative modelling error of Example 3.

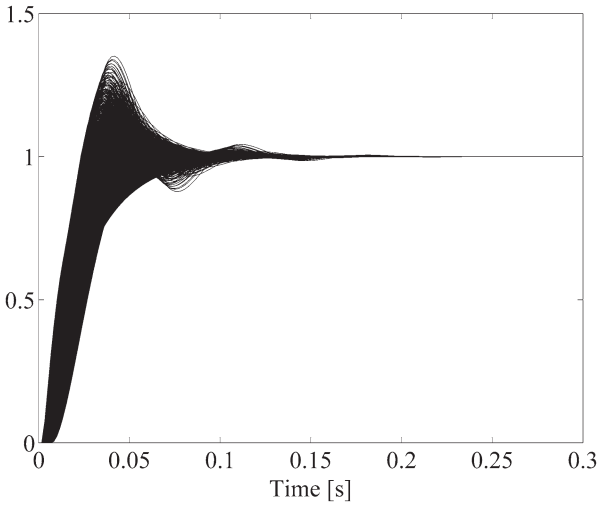

Figure 5. Velocity step responses with the parameter variations of Example 1.

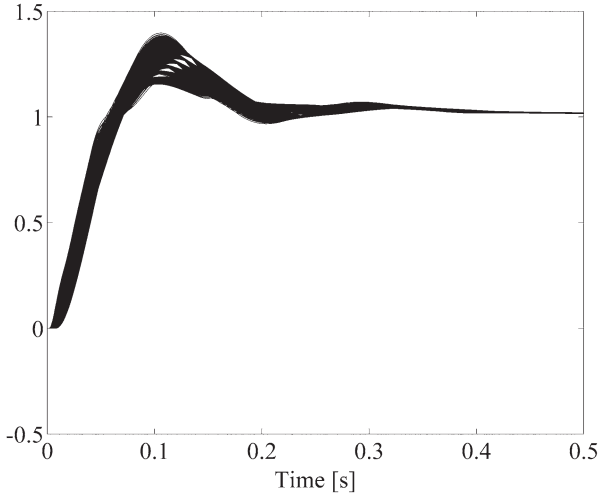

Figure 8. Position step responses with the parameter variations of Example 1.

2.6. Position tracking controller

The block diagram of the position controlled system is shown in Figure 6. The position loop design is similar to the velocity controller. The nominal open-loop transfer function is:

$$G_{N,\text{pos}} = \frac{G_N(s)G_V(s)}{s\big(1 + G_N(s)G_V(s)\big)} \tag{21}$$

and the true transfer function is:

$$G_{T,\text{pos}} = \frac{G_T(s)G_V(s)}{s\big(1 + G_T(s)G_V(s)\big)} \tag{22}$$

The multiplicative modelling error is:

$$\Delta_{\text{pos}}(s) = \frac{G_{T,\text{pos}}(s) - G_{N,\text{pos}}(s)}{G_{N,\text{pos}}(s)} \tag{23}$$

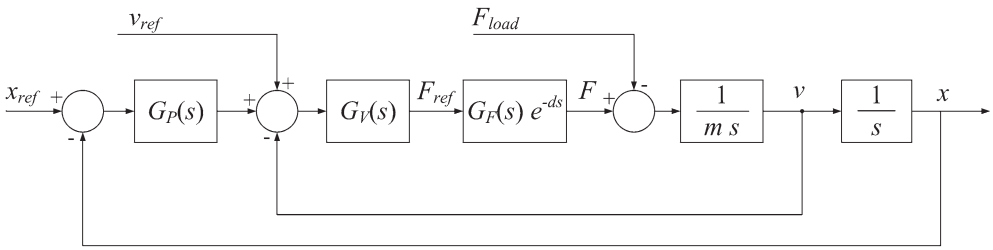

Figure 6. Block diagram of the position control system.

Analysis similar to Example 2 shows that the modified PID-controller is a good candidate for the position loop:

$$G_P(s) = \frac{K_{P,\mathrm{pos}}}{\tau_P s + 1} + \frac{K_{I,\mathrm{pos}}}{s} + \frac{K_{D,\mathrm{pos}} s}{\tau_D s + 1} \tag{24}$$

Example 3. Figure 7 shows the multiplicative modelling error of Equation 23 for the system presented in Examples 1 and 2. The parameter variations are the same as those in Example 1 and the velocity controller is tuned according to Example 2. Figure 7 also shows the term:

$$\left| \frac{1 + G_{N,\mathrm{pos}}(j\omega) G_P(j\omega)}{G_{N,\mathrm{pos}}(j\omega) G_P(j\omega)} \right| \tag{25}$$

when the controller parameters are $K_{P,\mathrm{pos}} = 32\ \mathrm{s}^{-1}$, $\tau_p = 15$ ms, $K_{I,\mathrm{pos}} = 120\ \mathrm{s}^{-2}$, $K_{D,\mathrm{pos}} = 0.4$, and $\tau_D = 2$ ms. Figure 8 shows the position step responses with different parameter values.

Example 3 shows that the integrator causes overshoot, but is essential in order to compensate for the force disturbances. The target is tracking control, and fast rise time and overall stability are more important than overshoot.

3. Simulation results

3.1. System model

The simulated system is a horizontal cylinder with a load mass ranging between 250 and 500 kg. The piston diameter is 40 mm, the piston rod diameter is 20 mm, and the stroke is 500 mm. The supply pressure is 10 MPa and the tank pressure is zero. The digital valve system consists of 4×16 miniaturized valves (Linjama *et al.* 2014). All the valves have the same flow capacity of 1.3 l/min at a 3.5 MPa pressure differential. The exponents are selected to be 0.53 and the cavitation choking parameters $\mathbf{b}_{\mathbf{PA}}(i)$, $\mathbf{b}_{\mathbf{AT}}(i)$, $\mathbf{b}_{\mathbf{PB}}(i)$ and $\mathbf{b}_{\mathbf{BT}}(i)$ are 0.3 for all of the valves. The valve delay is assumed to be 2.5 ms and the opening and closing happens with a linear motion profile within 1 ms. The friction force is modelled using the following equation:

$$F_\mu = \tanh\left(20000\ \mathrm{m}^{-1}\mathrm{s} \cdot \dot{x}\right) \left(280\ \mathrm{N} + 70\ \mathrm{N} \cdot e^{-10000\ \mathrm{m}^{-2}\mathrm{s}^2 \cdot \dot{x}^2}\right) + 100\ \mathrm{Nm}^{-1}\mathrm{s} \cdot \dot{x} \tag{26}$$

which is simplified version of the friction model presented by Makkar *et al.* (2005). The dead volumes V_{0A} and V_{0B} are 0.001 m^3, and the nominal value of the bulk modulus is 1200 MPa.

3.2. Implementation of position and velocity measurement

Real velocity is normally not measured but it is obtained from the measured position by differentiation. It is assumed that the position is measured by a pulse encoder with 0.01 mm resolution. The effect of quantization noise on velocity is reduced by using a filter suggested by Harrison and Stoten (1995):

$$\hat{x}(k) = \frac{5x(k) + 3x(k-1) + x(k-2) - x(k-3) - 3x(k-4) - 5x(k-5)}{35T_S} \tag{27}$$

The filter runs with 1 ms sampling period.

3.3. Force control results

The outer-loop controller of Equations 20 and 24 is disabled when the force tracking results are simulated. The sampling period of the controller is selected to be 4 ms, i.e. slightly more than the maximum response time of the valves. The weight factors $W_{u,p}$ and $W_{u,F}$ are selected such that the simultaneous opening of DFCUs PA and AT and DFCUs PB and BT is minimised, but the force tracking performance is still good. The values used are $W_{u,p} = 0.01$ MPa and $W_{u,F} = 2$ N. The estimate of the bulk modulus is selected to be 1500 MPa, which is considered to be the largest possible value. The parameter N_{cand} is selected to be six.

Figure 9 shows the simulated Bode diagram of the force controlled system when the load mass is 500 kg. The initial piston position is 0.2 m. The input signal is a sinusoidal force reference with 2 kN amplitude. The sinusoidal signal is fitted to the simulated force by using the least squares method and the magnitude ratio and phase shift are determined from the fitted curve. The −90° bandwidth is 180 rad/s for B = 700 MPa and 228 rad/s for B = 1200 MPa.

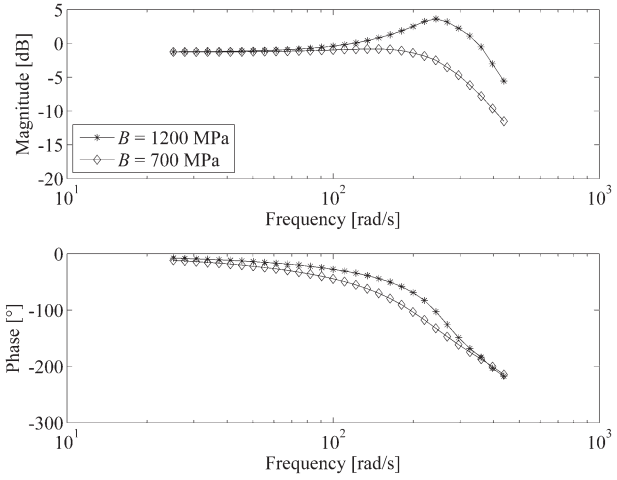

Figure 9. Simulated Bode diagrams of the force controller with a 500 kg load mass.

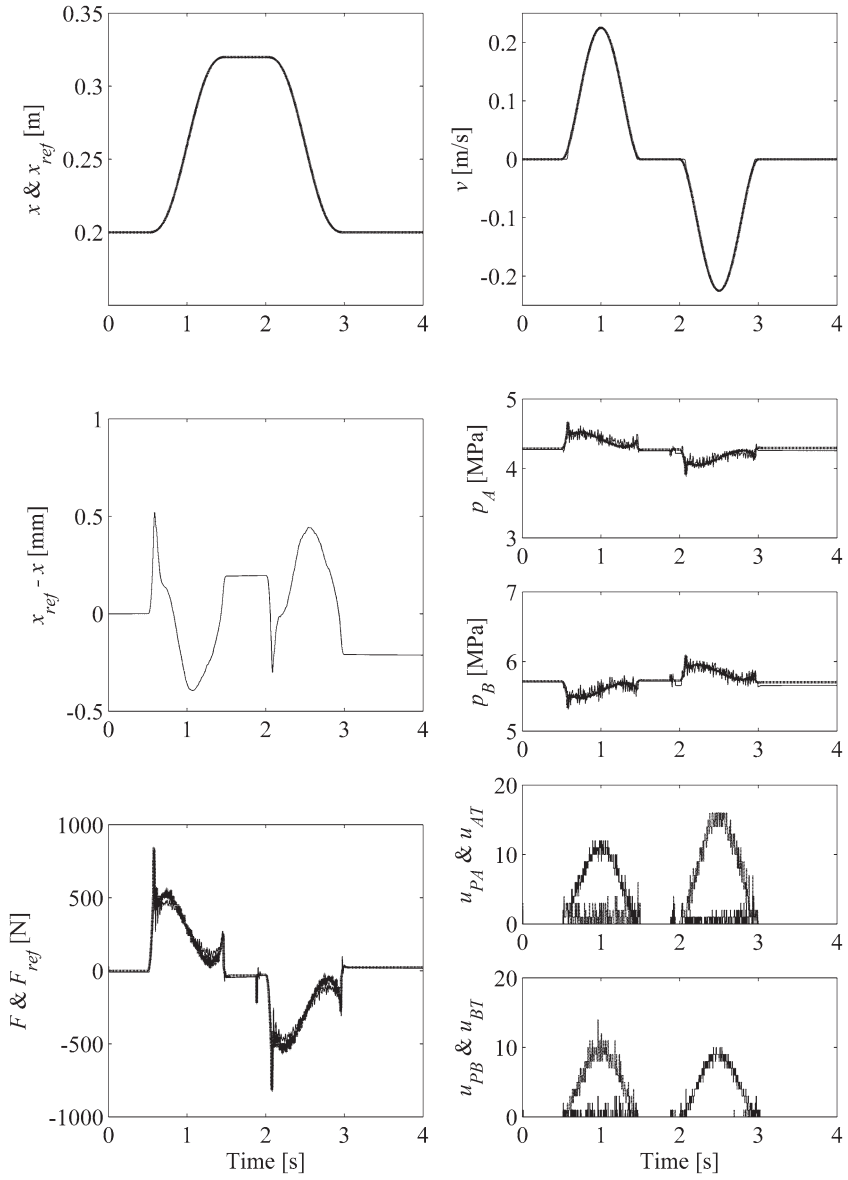

Figure 10. Position tracking results with a 250 kg load mass.

3.4. Position tracking results

The minimum load mass is assumed to be 250 kg. It is assumed that the true bulk modulus is at least 700 MPa, which results in a maximum time constant of 6.4 ms. The maximum system delay is assumed to be the 3 ms valve delay plus the sampling period, i.e. 7 ms. Thus, the parameters are the same as those found in Examples 1–3 and the resulting tuning is $K_{P,\mathrm{vel}}$ = 19000 Ns/m, $K_{P,\mathrm{pos}} = 32\ \mathrm{s}^{-1}$, $\tau_p = 15$ ms, $K_{I,\mathrm{pos}} = 120\ \mathrm{s}^{-2}$, and $K_{D,\mathrm{pos}} = 0.4$. The derivative of the error signal is formed by equation 27. The integrator term has a ±0.3 mm dead zone in order to avoid the limit cycles. The error signal of the integrator term is calculated as follows:

$$e_I = \begin{cases} e\ , & |e| \geq \text{deadzone} \\ 0\ , & |e| < \text{deadzone} \end{cases} \tag{28}$$

The estimate of the friction force is added to the force reference and is calculated as follows:

$$\hat{F}_\mu = 250\ \mathrm{N} \cdot \tanh\left(20000\ \mathrm{m}^{-1}\mathrm{s} \cdot \dot{x}\right) \tag{29}$$

The estimate is smaller than real friction in order to guarantee stability at zero velocity. Figure 10 presents the simulated response with a 250 kg load mass. The position trajectory is the fifth order polynomial with 120 mm amplitude and 1 s movement time. The peak velocity is 225 mm/s and the maximum position tracking error is 0.52 mm. Thus, the performance index is 0.0023 s. The plots also show that the pressure and force tracking are reasonable.

Figure 11 depicts the simulated response when the load mass is increased to 500 kg. The tracking error increases to 0.73 mm and the performance index increases to 0.0032 s.

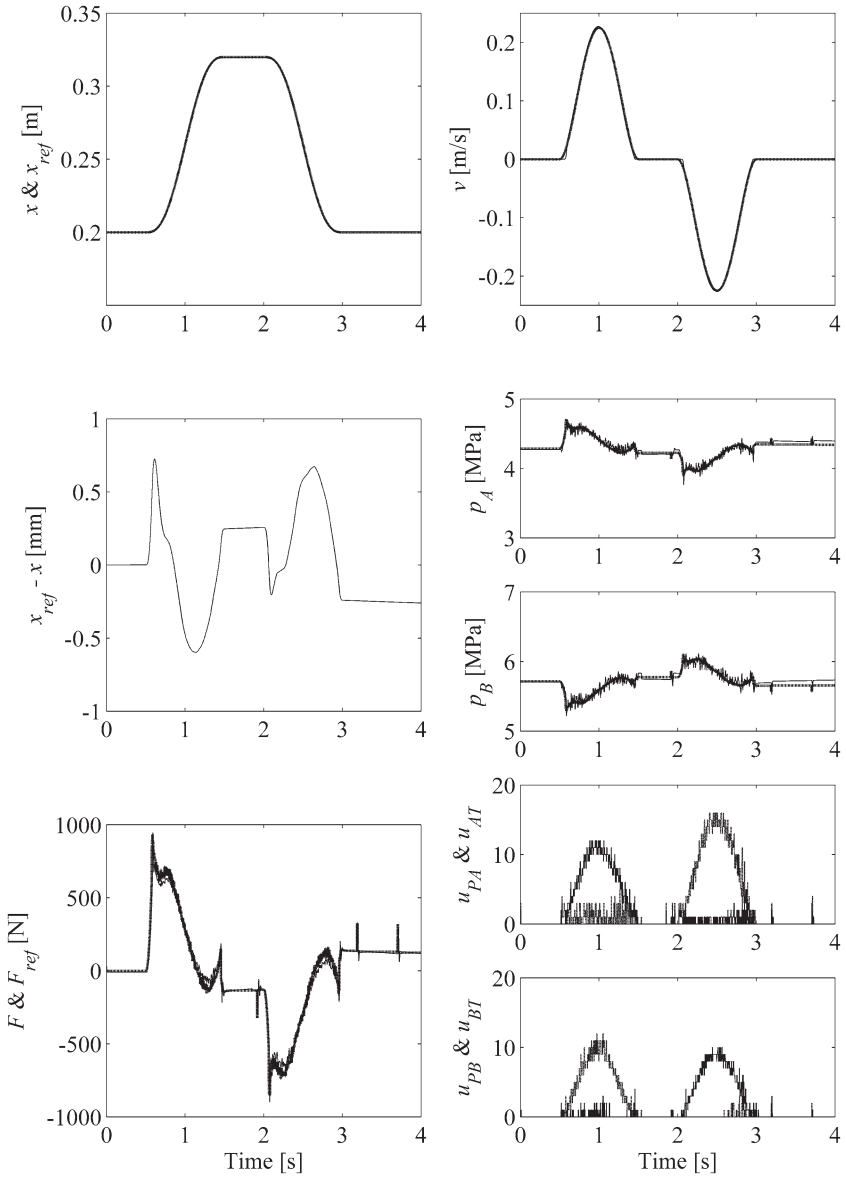

Figure 11. Position tracking results with a 500 kg load mass.

4. Conclusions

This paper has presented a new digital hydraulic tracking control solution for systems with big inertia. The parameter uncertainty is expressed as the unstructured multiplicative error and the low-order controllers are tuned in order to achieve robust stability. The core component of the controller is the model-based force controller, which allows force tracking under unknown bulk modulus. The suggested outer loop P + modified PID cascade controller results in good position tracking performance under unknown load mass, bulk modulus, and system delay. The simulated maximum position tracking error is 0.73 mm while the maximum piston velocity is 225 mm/s. The relative accuracy (tracking error divided by peak velocity) is comparable to more advanced control solutions. The suggested controller needs pressure, position, and velocity measurements but not derivatives of those. Moreover, when comparing the performance against other controller solutions it must be noted that the solution presented in this paper does not require exact knowledge of inertia, delay, or bulk modulus.

Nomenclature

A_A	Piston area, piston side [m^2]
A_B	Piston area, rod side [m^2]
$\mathbf{b}$	Vector of relative sizes of valves of DFCUs
$\mathbf{b}_{XY}$	Vector of critical pressure ratios of valve model of DFCU XY, where XY is either PA, AT, PB or BT [–]
B_A, B_B	Bulk moduli of A- and B-side chambers [Pa]
d	System delay [s]
$d_{\min}$	Minimum system delay [s]
e	Position error [m]
e_I	Position error used by integrator term [m]
F_{load}	External force [N]
F_{ref}	Target force [N]
F_μ	Friction force [N]

$G_F(s)$	Transfer function from F_{ref} to force
$G_N(s)$	Nominal transfer function from force to velocity
$G_{N,\text{pos}}(s)$	Nominal transfer function from force to position
$G_p(s)$	Transfer function from supply and tank pressure to force
$G_p(s)$	Transfer function of the position controller
$G_T(s)$	True transfer function from force to velocity
$G_{T,\text{pos}}(s)$	True transfer function from force to position
$G_V(s)$	Transfer function of the velocity controller
J	Cost function for force error [N]
J_A	Cost function for A-side pressure error [Pa]
J_B	Cost function for B-side pressure error [Pa]
K	Parameter of multiplicative modelling error limit
$K_{D,\text{pos}}$	Position controller gain, D-term [–]
$K_{I,\text{pos}}$	Position controller gain, I-term [s^{-2}]
$K_{P,\text{pos}}$	Position controller gain, P-term [s^{-1}]
$K_{P,\text{vel}}$	Velocity controller gain [N $m^{-1}s$]
$\mathbf{K_{v,XY}}$	Vector of flow coefficients of valve model of DFCU XY, where XY is either PA, AT, PB or BT [$m^3s^{-1}Pa^x$]
m	Load mass [kg]
m_{min}	Minimum load mass [kg]
N	Number of parallel connected valves
N_{cand}	Number of control candidates for A- and B-side
p_A	Pressure at A-chamber [Pa]
$p_{A,\text{ref}}$	Target value for A-pressure [Pa]
p_B	Pressure at B-chamber [Pa]
$p_{B,\text{ref}}$	Target value for B-pressure [Pa]
p_P	Supply pressure [Pa]
p_T	Tank line pressure [Pa]
Q_{AT}	Flow rate from A-chamber to tank line [m^3/s]
Q_{BT}	Flow rate from B-chamber to tank line [m^3/s]
Q_{PA}	Flow rate from supply line to A-chamber [m^3/s]
Q_{PB}	Flow rate from supply line to B-chamber [m^3/s]
T_S	Sampling period of the controller [s]
$\mathbf{u_{XY}}$	Vector of control signals of valves of DFCU XY, where XY is either PA, AT, PB or BT [–]
V_{0A}	A-side dead volume [m^3]
V_{0A}	B-side dead volume [m^3]
$W_{u,F}$	Weight for openings of DFCUs [N]
$W_{u,p}$	Weight for openings of DFCUs [Pa]
x	Piston position [m]
x_{max}	Maximum piston position [m]
$\mathbf{x_{XY}}$	Vector of exponents of valve model of DFCU XY, where XY is either PA, AT, PB or BT [–]
Δ	Multiplicative modelling error, velocity loop
Δ_M	Limit for multiplicative modelling error
Δ_{pos}	Multiplicative modelling error, position loop
τ	Parameter of multiplicative modelling error limit
τ_A	Time constant of A-side pressure dynamics [s]
τ_B	Time constant of B-side pressure dynamics [s]
τ_D	Time constant of derivative term
$\hat{\bullet}$	Estimate of $\bullet$

Disclosure statement

No potential conflict of interest was reported by the authors.

Funding

This work was supported by the Academy of Finland; Luonnontieteiden ja Tekniikan Tutkimuksen Toimikunta [grant number 286401].

Notes on contributors

Matti Linjama is Adjunct Professor at the Tampere University of Technology. He leads the digital hydraulics research group at the Department of Intelligent Hydraulics and Automation.

Mikko Huova has just finished his PhD thesis about energy efficient digital hydraulic valve control and works as a senior researcher in the digital hydraulics research group.

Kalevi Huhtala is head of the Department of Intelligent Hydraulics and Automation. He is a professor of mobile machines.

References

Eryilmaz, B. and Wilson, B.H., 2001. Improved tracking control of hydraulic systems. *Journal of dynamic systems, measurement, and control*, 123, 457–462.

Goode, S., 2000. *Differential equations and linear algebra*. 2nd ed. Upper Saddle River, NJ: Prentice Hall.

Green, M. and Limebeer, D., 1995. *Linear robust control*. Englewood Cliffs, NJ: Prentice Hall.

Harrison, A. and Stoten, D., 1995. Generalized finite difference methods for optimal estimation of derivatives in real-time control problems. *Proceedings of the institution of mechanical engineers, part I: journal of systems and control engineering*, 209, 67–78.

Jelali, M. and Kroll, A., 2004. *Hydraulic servo-systems, modelling, identification and control*. London: Springer-Verlag.

Kim, W., Won, D., and Tomizuka, M., 2015. Flatness-based nonlinear control for position tracking of electrohydraulic

systems. *IEEE/ASME transactions on mechatronics*, 20 (1), 197–206.

Koivumäki, J. and Mattila, J., 2015. High performance nonlinear motion/force controller design for redundant hydraulic construction crane automation. *Automation in construction*, 51, 59–77.

Linjama, M. and Vilenius, M., 2005. Improved digital hydraulic tracking control of water hydraulic cylinder drive. *International journal of fluid power*, 6 (1), 29–39.

Linjama, M., *et al*., 2008. Comparison of digital hydraulic and traditional servo system in demanding water hydraulic tracking control. *In*: D.N. Johnston and A.R. Plummer, eds. *Fluid power and motion control (FPMC 2008)*, 10–12 September 2008 bath. Basildon: Hadleys, 393–403.

Linjama, M. and Vilenius, M., 2008. Digital hydraulics: towards perfect valve technology. *Ventil, Revija za Fluidno Tehniko, Avtomatizacijo in Mehatroniko*, 14 (2), 138–148.

Linjama, M., Huova, M., and Karvonen, M., 2012. Modelling of flow characteristics of on/off valves. *Proceedings of the fifth workshop on digital fluid power*, 24–25 October 2012 Tampere, Finland. Tampere: Tampere University of Technology, 209–222.

Linjama, M., Paloniitty, Tiainen, L. and Huhtala, K., 2014. Mechatronic design of digital hydraulic micro valve package. *The second international conference on dynamics and vibroacoustics of machines*, 15–17 September 2014 Samara, 610–617.

Makkar, C., *et al*., 2005. A new continuously differentiable friction model for control systems design. *The 2005 IEEE/ASME international conference on advanced intelligent mechatronics*, 24–28 July 2005 Monterey, 600–604.

Won, D., *et al*., 2015. High-gain disturbance observer-based backstepping control with output tracking error constraint for electro-hydraulic systems. *IEEE transactions on control systems technology*, 23 (2), 787–795.

Zhu, W.-H. and Vukovich, G., 2011. Virtual decomposition control for modular robot manipulators. *IFAC world congress*, 28 August–2 September 2011 Milano, 13486–13491.